Supporting Information

Modulation of Lanthanide Luminescence via Electric Field

Yangbo Wang[1,3], Jiaxin Gao[1], Chao Gao[1], Hui Ma[1], Bingxiao Yang[1], Yingdong Han[1,4], Enlong Zhou[1], Qianya Cheng[2], Su Jing[2], and Ling Huang[1]**

[1]Y. Wang, J. Gao, C. Gao, H. Ma, Dr. B. Yang, Dr. Y. Han, Dr. E. Zhou, and Prof. L. Huang
Institute of Advanced Materials, Nanjing Tech University, 30 South Puzhu Road, Nanjing 211816 China
E-mail: iamlhuang@njtech.edu.cn

[2]Q. Cheng, and Prof. S. Jing
School of Chemistry and Molecular Engineering, Nanjing Tech University, 30 South Puzhu Road, Nanjing 211816 China
E-mail: sjing@njtech.edu.cn

[3]Dr. Y. Wang
School of Materials Science and Engineering, Liaocheng University, 1 Hunan Road, Liaocheng 252059, China

[4]Dr. Y. Han
School of Precision Instrument and Opto-Electronics Engineering, Tianjin University, 92 Weijin Road, Tianjin 300072, China

Keywords: semiconductor nanocrystals, photoluminescence, modulation, lanthanide, electric field

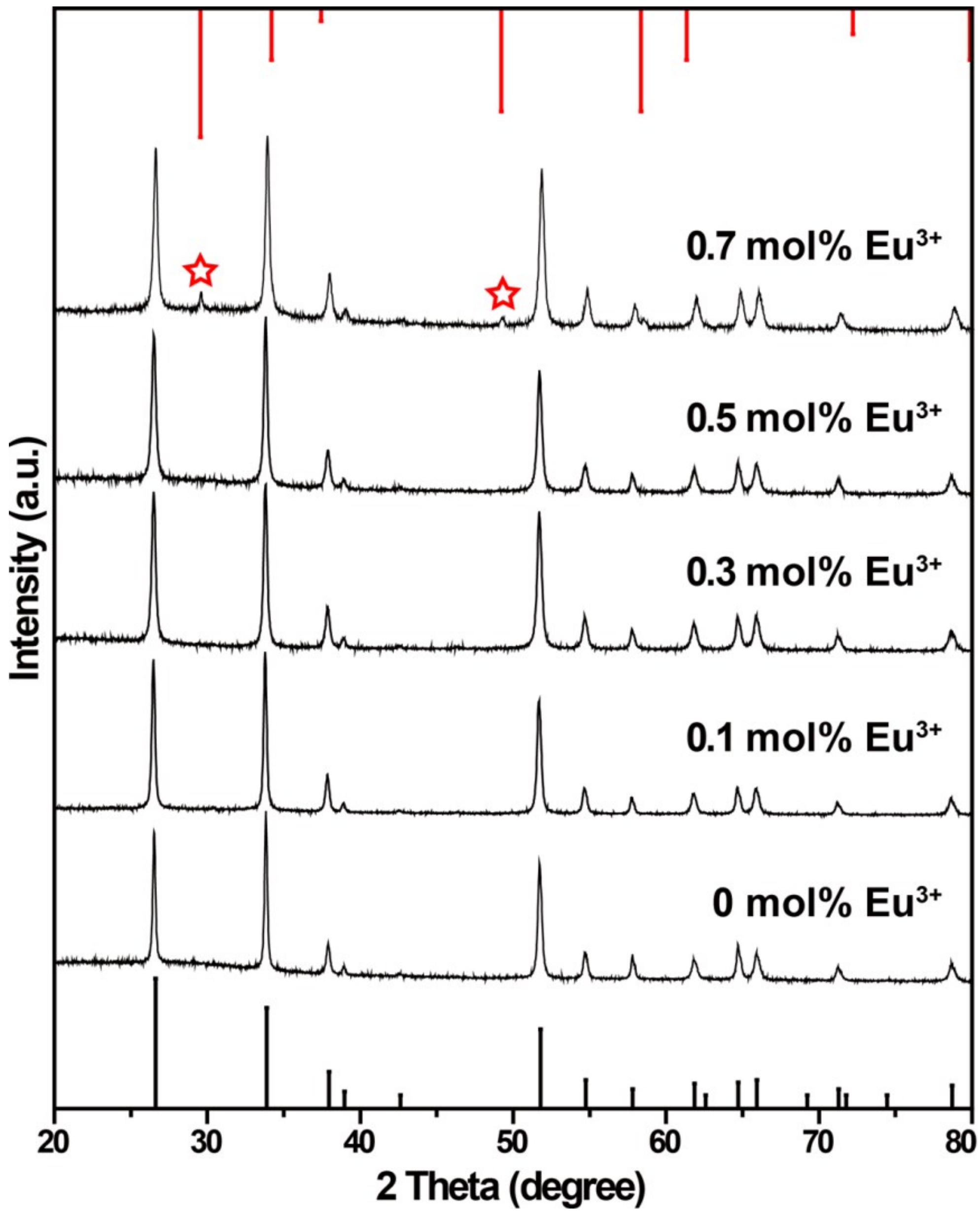

Figure S1. XRD patterns of SnO_2:Eu nanocrystals doped with 0, 0.1, 0.3, 0.5, and 0.7 mol% Eu^{3+}, respectively. The black and red bars represent the standard XRD patterns of tetragonal SnO_2 (JCPDS: 41-1445) and cubic $Eu_2Sn_2O_7$ (JCPDS: 13-0182), respectively. The peaks intentionally marked with red stars represent the $Eu_2Sn_2O_7$ phase.

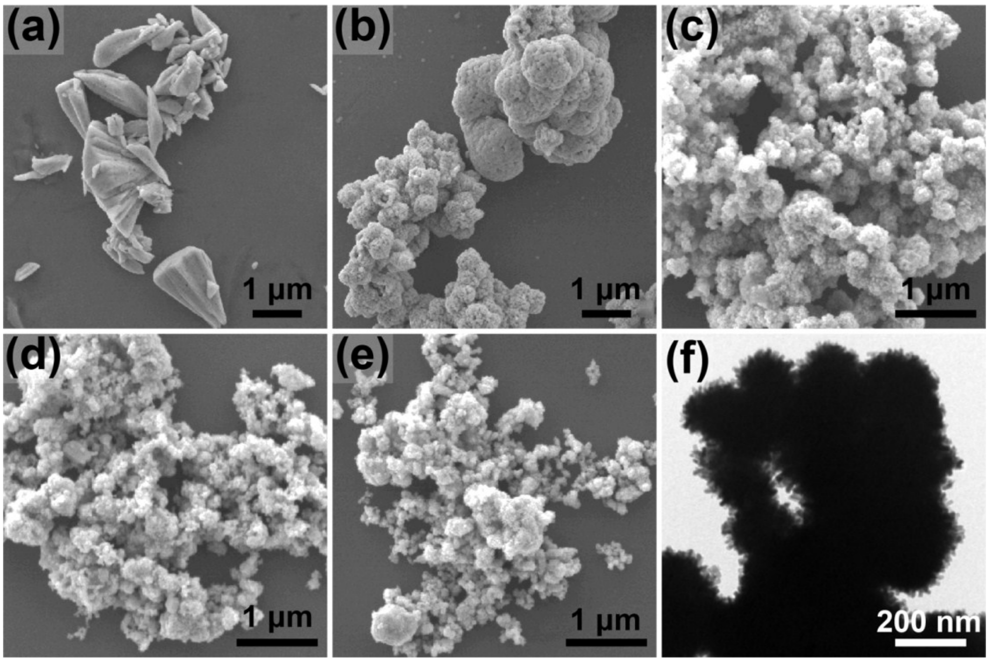

Figure S2. SEM images of SnO_2:Eu nanocrystals doped with (a) 0, (b) 0.1, (c) 0.3, (d) 0.5, and (e) 0.7 mol% Eu^{3+}, respectively. TEM image (f) of SnO_2:Eu (0.5 mol%) nanocrystals.

Table S1 Elemental analysis of SnO_2:Eu nanocrystals doped with 0.1, 0.3, and 0.5 mol% Eu^{3+}.

Eu^{3+} Doping (mol%)	Eu^{3+} Detected (mol%)
0.1	0.11
0.3	0.27
0.5	0.39

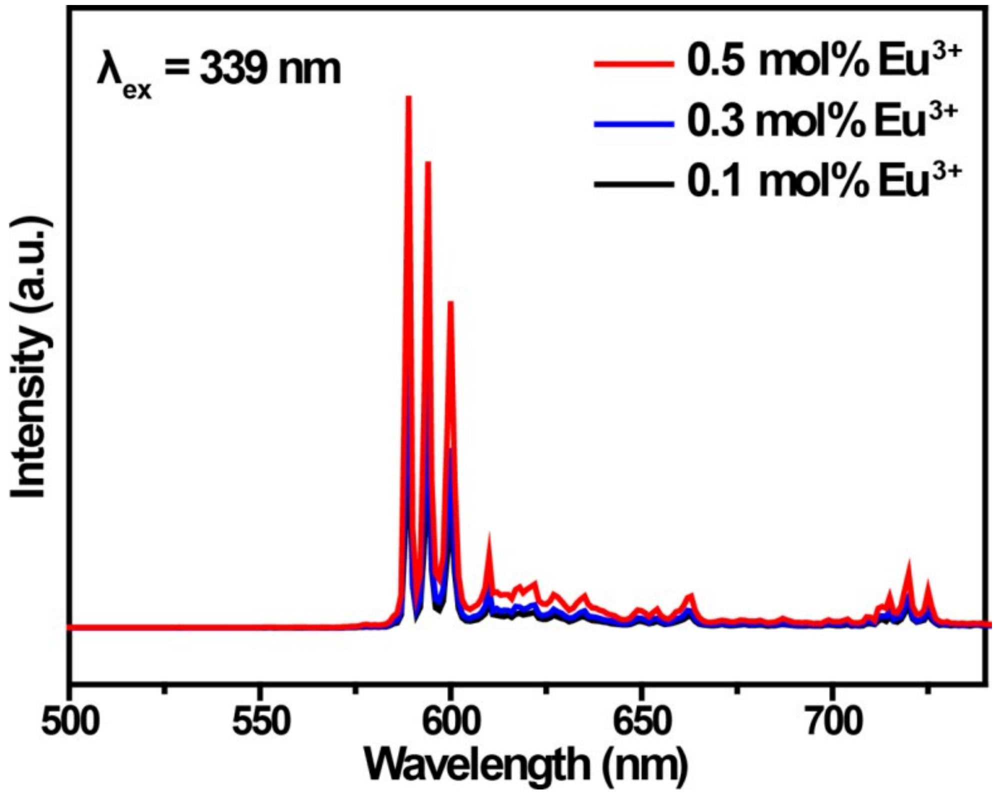

Figure S3. Photoluminescence spectra of SnO_2:Eu nanocrystals doped with 0.1, 0.3, and 0.5 mol% Eu^{3+}, respectively, and under 339 nm UV light excitation.

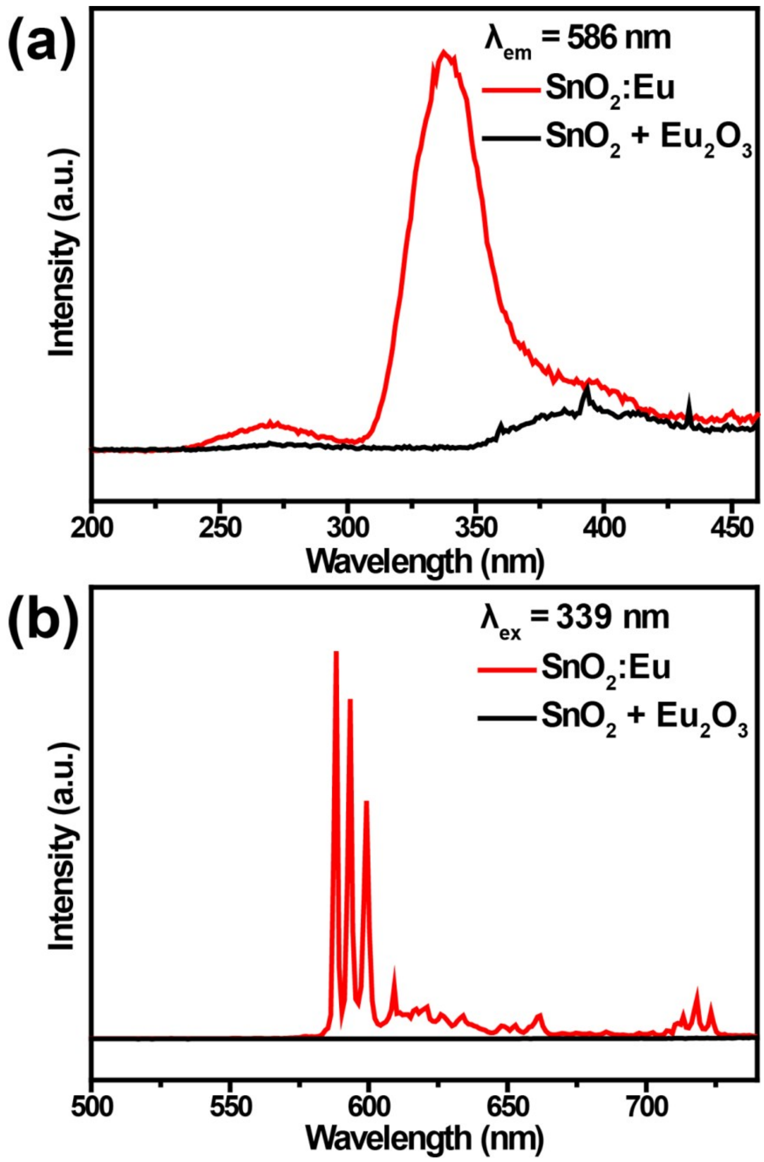

Figure S4. (a) Excitation and (b) emission spectra of SnO_2:Eu (0.5 mol%) nanocrystals and the mixture of SnO_2 and Eu_2O_3 at atom ratio [Eu/(Eu + Sn)] of 0.5%, the mixture was ground several times for good uniformity.

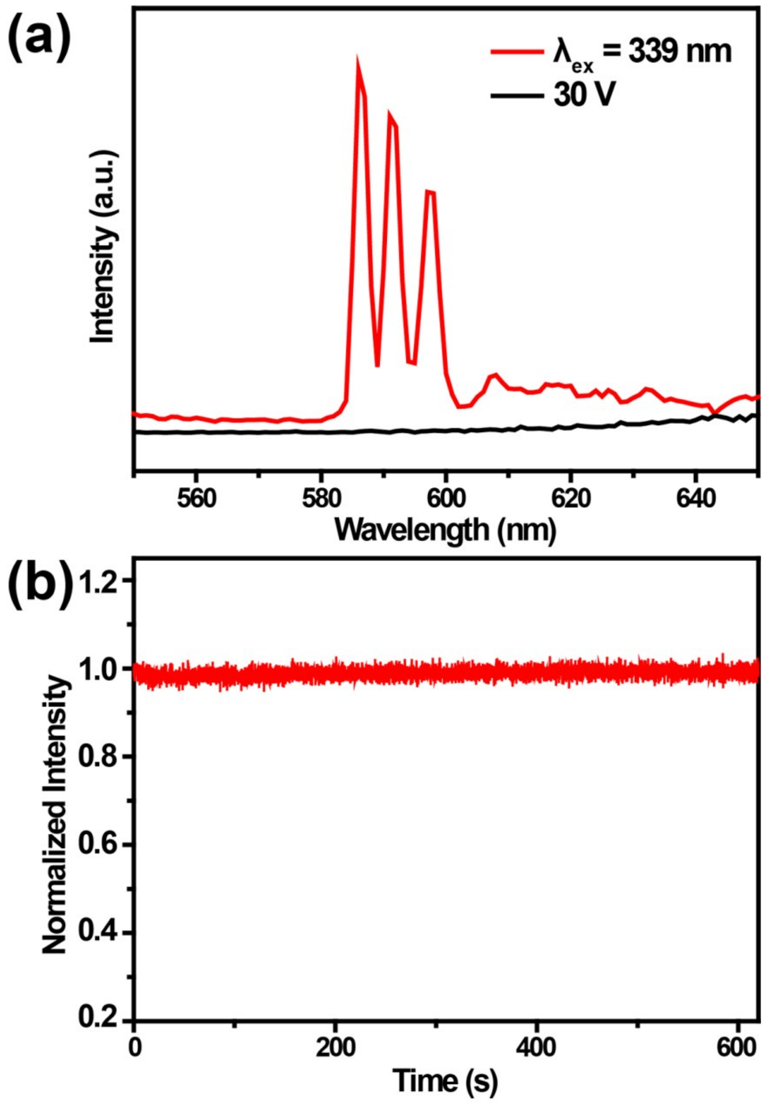

Figure S5. (a) Emission spectra of SnO_2:Eu (0.5 mol%) nanocrystals under 339 nm UV light excitation or 30 V dc voltage, respectively. (b) Photoluminescence intensity of SnO_2:Eu (0.5 mol%) nanocrystals at 586 nm under 339 nm UV light excitation to exclude the influence of prolonged illumination time on luminescence intensity.

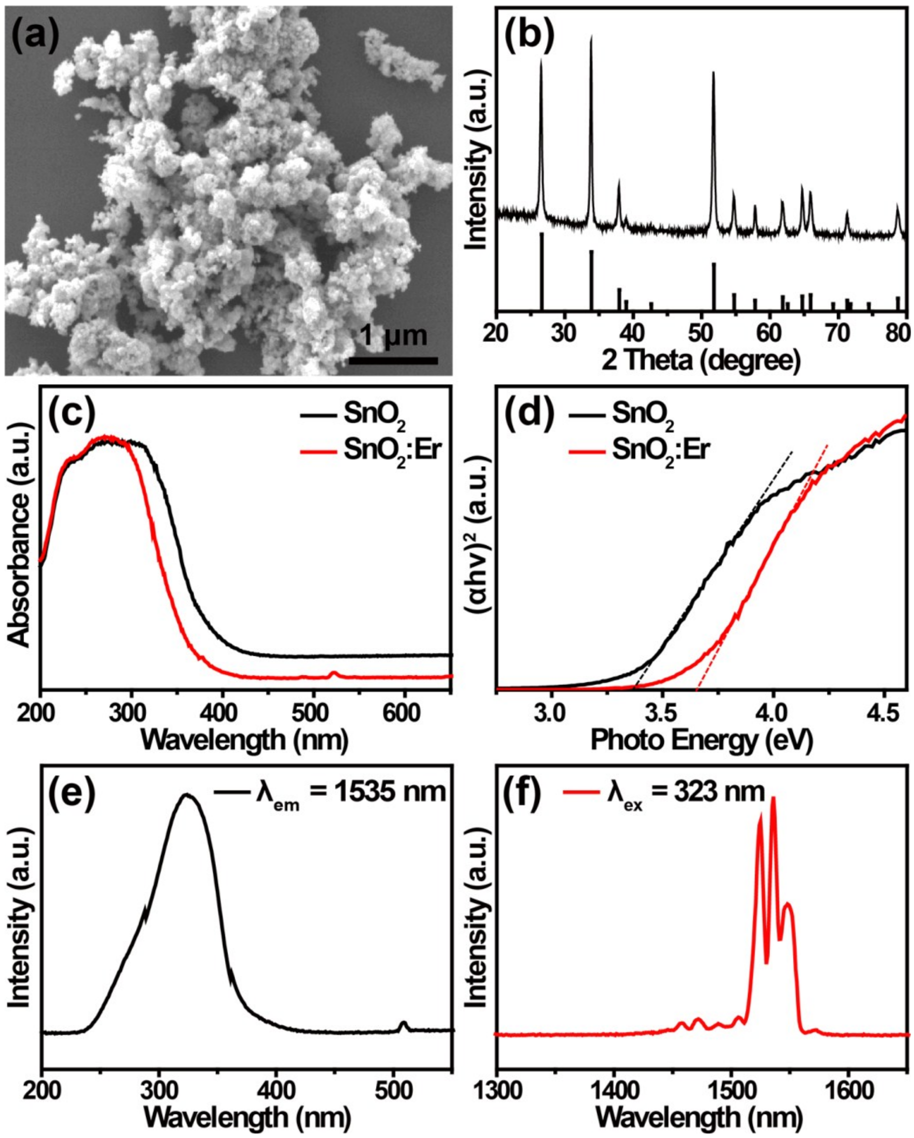

Figure S6. (a) SEM image and (b) XRD patterns of SnO_2:Er (0.5 mol%) nanocrystals. The black bars in (b) represent the standard XRD patterns of tetragonal SnO_2 (JCPDS: 41-1445). (c) UV-vis absorption spectra and (d) plot of $(\alpha h\nu)^2$ versus photo energy ($h\nu$) of SnO_2 and SnO_2:Er (0.5 mol%) nanocrystals. (e) Excitation and (f) emission spectra of SnO_2:Er (0.5 mol%) nanocrystals.

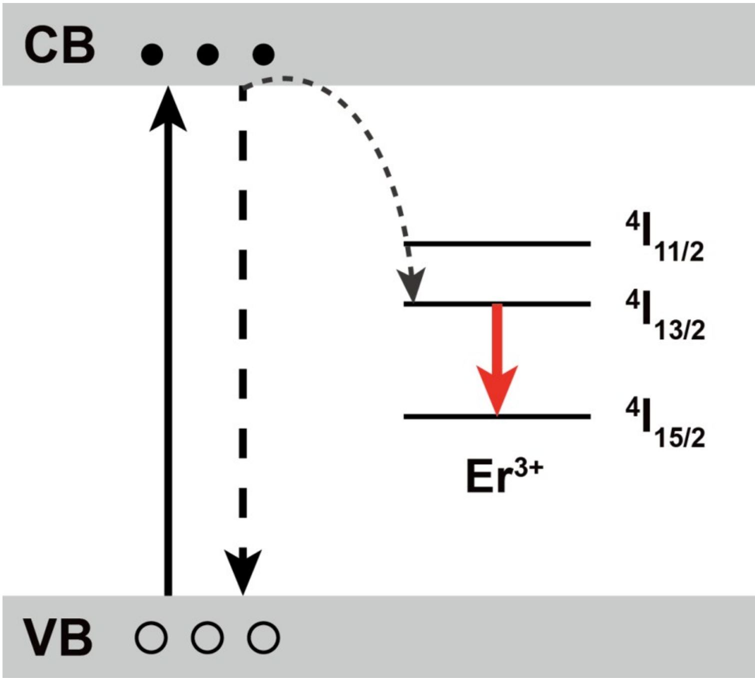

Figure S7. Energy transfer mechanism from SnO_2 host to Er^{3+} doped inside.

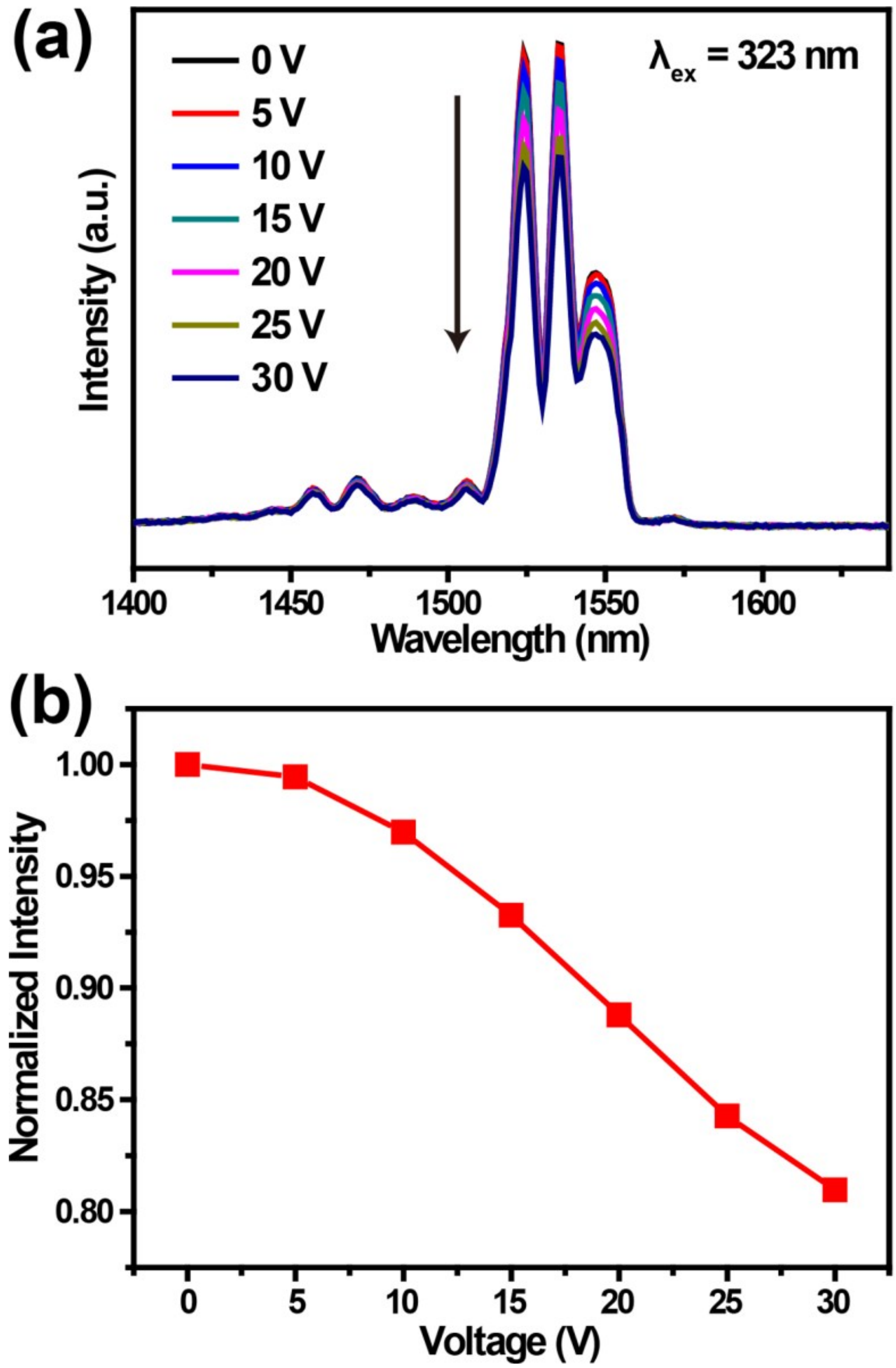

Figure S8. In-situ (a) photoluminescence spectra and (b) emission intensity variation (1500-1600 nm) of SnO_2:Er (0.5 mol%) nanocrystals as a function of applied dc voltages, under 323 nm UV light excitation.

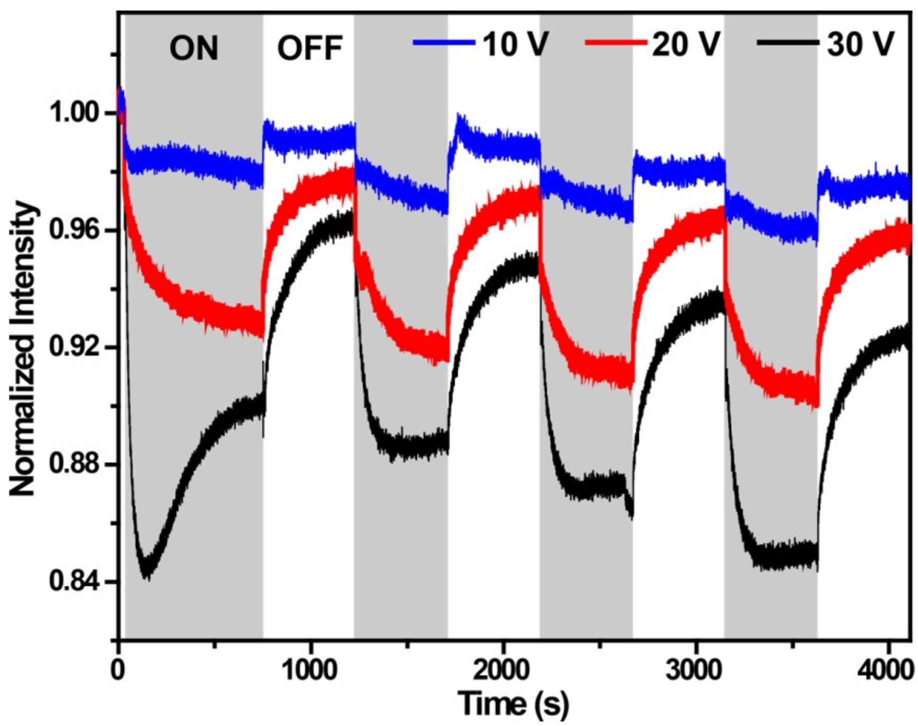

Figure S9. In-situ photoluminescence intensity variation at 1535 nm of SnO_2:Er (0.5 mol%) nanocrystals follows the ON/OFF of applied dc voltage (10, 20 and 30 V), under 323 nm UV light excitation.

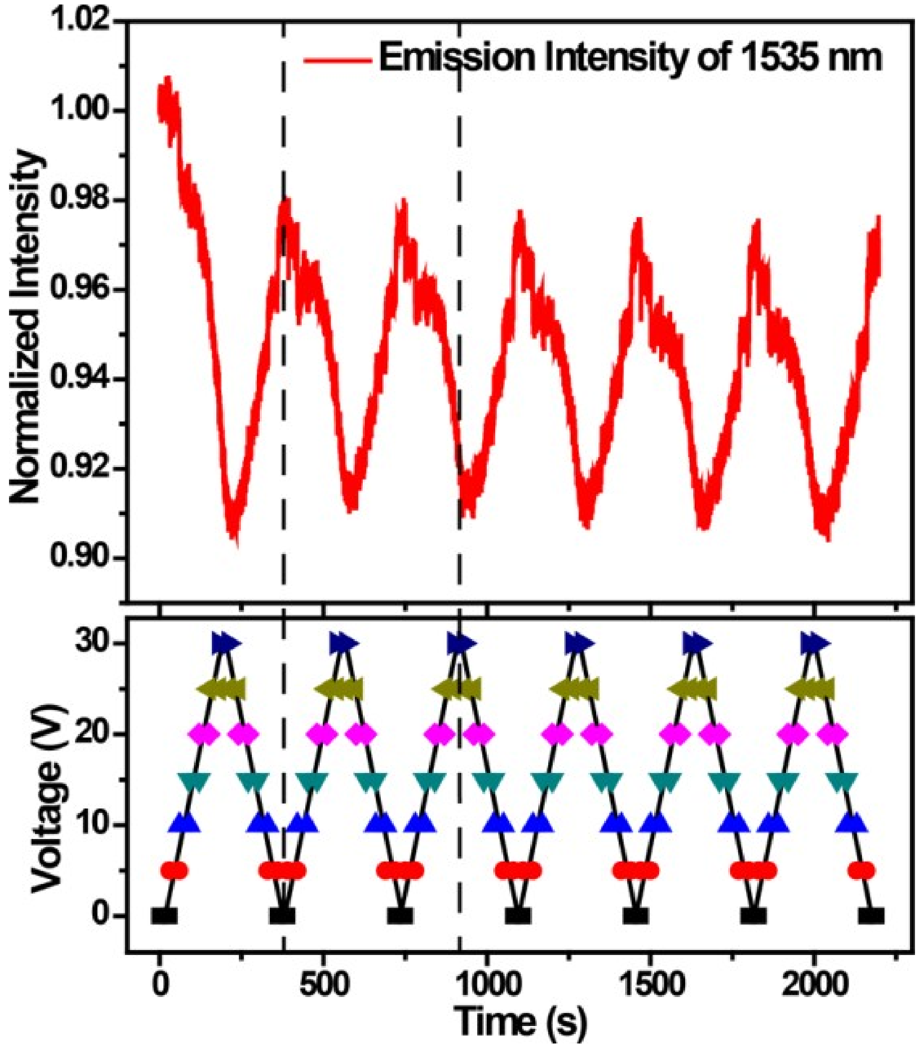

Figure S10. In-situ photoluminescence intensity variation at 1535 nm of SnO_2:Er (0.5 mol%) nanocrystals as a function of voltage, under 323 nm UV light excitation.

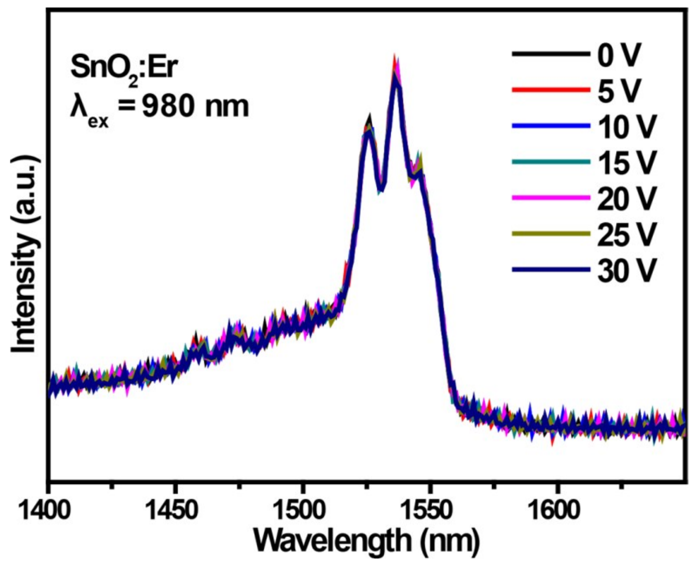

Figure S11. In-situ photoluminescence spectra of SnO_2:Er nanocrystals at varying dc voltages, under 980 nm laser excitation.

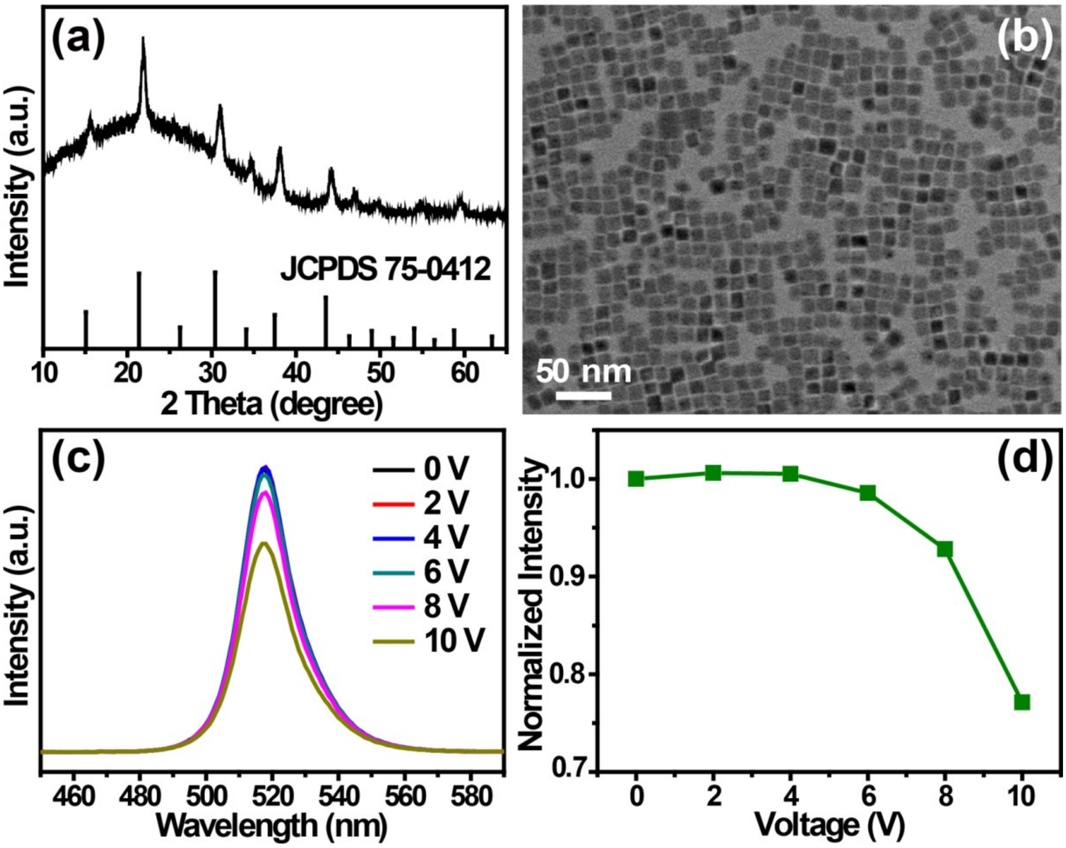

Figure S12. (a) XRD pattern and (b) TEM image of the synthesized $CsPbBr_3$ nanocrystals. The bars in the bottom in (a) represent the standard XRD patterns of cubic $CsPbBr_3$ (JCPDS: 75-0412). (c) In-situ photoluminescence spectra and (d) emission intensity variation of $CsPbBr_3$ nanocrystals as a function of applied dc voltages, under 365 nm UV light excitation.